



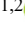




Evaluation of EnMAP Hyperspectral Data for the Identification of Placers in the Rias Baixas Region (Spain)

Beatriz L. Araújo¹^a, Joana Cardoso-Fernandes^{1,2}^b, Antonio Azzalini¹^c, Morgana Carvalho^{1,2}^d, Alexandre Lima^{1,2}^e, Francisco J. González³^f and Ana Cláudia Teodoro^{1,2}^g

¹Department of Geosciences, Environmental and Spatial Planning, Faculty of Sciences of the University of Porto, Rua do Campo Alegre s/n, Porto, Portugal

²ICT (Institute of Earth Sciences) – Porto Pole, Portugal

³Marine Geology Resources and Extreme Environments, Geological Survey of Spain (IGME-CSIC), Madrid, Spain

Keywords: Vigo, CRMs, Heavy-Mineral, Placers, EnMAP, Band Ratios, Spectral Unmixing, MTMF, Remote Sensing.

Abstract: Critical Raw Materials are crucial to achieve the European Union's (EU) goals of a climate-neutral economy by 2050. The high supply risk led the EU to prioritise domestic mineral exploration. This study, part of the S34I – SECURE AND SUSTAINABLE SUPPLY OF RAW MATERIALS project, utilised remote-sensing-based methods to identify and map heavy-mineral (HM) placer deposits in the Ria de Vigo, located in Galicia, Spain. Documented since the 70s, the sands of the Vigo beaches contain placers rich in Ti, Sn, Li, Rare Earth Elements (REE), Au, Fe and Cu. Mineral mapping was performed using hyperspectral EnMAP data. Band ratios were applied to identify possible mineralisation areas. Additionally, spectral unmixing was performed through the Mixture Tuned Matched Filtering (MTMF) workflow, included in ENVI 6.0 software, and two classification maps were obtained: one utilising the USGS spectral library and the other employing an HM concentrate spectral library. Band ratios were able to distinguish possible areas of hydrothermal alteration. MTMF classifications mapped most HM known to occur in the Ria, namely sillimanite, garnet, tourmaline, ilmenite, rutile, and monazite, were identified. This first approach will allow the selection of areas of interest for field validation and verification. The results will also be confronted with existing geological data.


1 INTRODUCTION


Critical Raw Materials (CRMs) are vital in key industries, such as renewable energy, electronics, defence and space exploration (Hool et al., 2023). These materials are crucial for achieving the European Union (EU) goals of a climate-neutral economy by 2050 and supporting the green and digital transition (European Commission et al., 2023)


The S34I – Secure and Sustainable Supply of Raw Materials for EU Industry project, funded by the European Union under grant agreement no.


101091616 (<https://doi.org/10.3030/101091616>), addresses these European needs through the development of data-driven methods to analyse Earth Observation (EO) data to support mineral exploration and monitoring of the complete mining cycle in its exploration, closure and post-closure phases. This project aims to enhance EU autonomy regarding CRMs, support the green transition, as well as address environmental challenges within the mining cycle.


To contribute to those goals, this work applied remote sensing techniques and hyperspectral data to identify Heavy Mineral (HM) beach placer deposits


^a <https://orcid.org/0000-0002-5734-6155>


^b <https://orcid.org/0000-0001-8265-3897>

^c <https://orcid.org/0000-0003-1058-5463>

^d <https://orcid.org/0000-0001-9920-0886>

^e <https://orcid.org/0000-0002-6598-5934>

^f <https://orcid.org/0000-0002-6311-1950>

^g <https://orcid.org/0000-0002-8043-6431>

in the Ria de Vigo, located in the Rias Baixas region, Spain. These HM placer deposits, known to occur in this region since the 70s (IGME, 1976), are rich in Ti, Sn, Li, Rare Earth Elements (REE), Au, Fe and Cu – some of which are classified as CRMs by the European Commission.

Several studies concerning the identification and characterisation of HM placer deposits using remote sensing have been carried out using multiple approaches.

Chandrasekar et al. (2011) used Landsat 7 Enhanced Thematic Mapper Plus data and the Environment for Visualising Images (ENVI) software to successfully map minerals like garnet, zircon and monazite along India's South Tamil Nadu coast. Gazi et al. (2019) similarly used Landsat 8, ENVI, ArcGIS and Erdas Imagine software to identify and determine the concentration of HM placer deposits on the Cox Bazar beaches. Rejith et al. (2020) utilised ASTER and Landsat 8 data to map beach sediments on the coast of Thiruvananthapuram, India, by applying the Spectral Angle Mapper algorithm (SAM). Later, Rejith et al. (2022) also mapped and studied the beach placers on the east coast of Nadu, India, using EO-1 Hyperion data and employing SAM image classification and Random Forest regression.

In this study, we made a first approach to the use of hyperspectral Environmental Mapping and Analysis Program (EnMAP) data used for mineral mapping to evaluate the potential of such data for placer exploration.

2 STUDY AREA

The Rias Baixas region is located on the Atlantic margin of southwestern Galicia, in north-western Spain, close to the border with Portugal (Fig. 1). It is composed of four morphologically identical estuaries, known as Rias, of which the Ria de Vigo, the target of this study, is the southernmost.

The Ria de Vigo is 32.5 km long, measuring 1 km in width at its inner part, gradually expanding as it extends towards the mouth of the Ria, where it becomes 10 km wide, and therefore exhibiting a distinctive funnel-shaped morphology, positioned with a NE-SW direction (Méndez & Vilas, 2005).

The geology of this region, which is a part of the Galicia Trás-os-Montes zone of the Iberian Massif, consists mainly of metasedimentary sequences, amphibolites, gneisses and Variscan granitoids (Capdevila & Floor, 1970; Julivert et al., 1974; Navas & Corretgé, 1997) (Fig. 2). The geological,

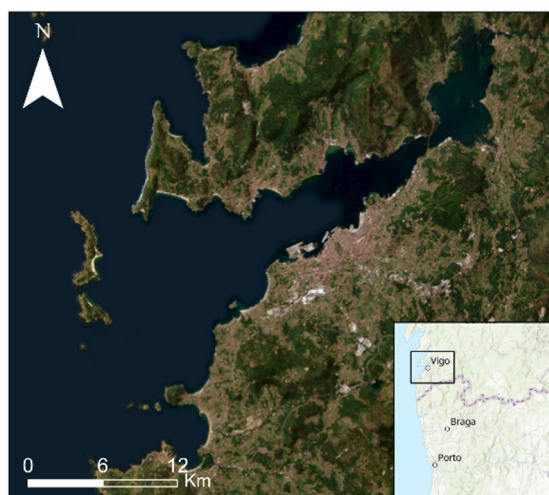


Figure 1: Geographical location of the Ria de Vigo in Galicia, Spain.

geomorphological and hydrodynamic characteristics of the Galician beaches allow for concentration of economically valuable HM, such as magnetite, ilmenite, garnet, zircon, cassiterite, monazite and spodumene, forming placer deposits in the land-sea transition and shallow waters (Galván, 2002; Gent et al., 2005; IGME, 1976; Méndez et al., 2000; Pérez et al., 2008; Prego et al., 2009).

The HM sands form elongated layers aligned parallel to the coastline and are present in Límens, Santa Marta, Alemáns, Canabal, Ratas, Patos and Vao beaches. These placer deposits vary seasonally due to changes in the hydrographic conditions of the Ria. In late summer and early autumn, HM accumulation is higher in the Ria's northern margin, while in late winter and early spring, it is higher in the southern margin (Ng-Cutipa et al., 2024).

3 DATA AND METHODS

3.1 Data

For mineral mapping, EnMAP data was employed. The EnMAP image, a Level-2A product consisting of 224 spectral bands (out of the original 246), was acquired on 26 June 2024 with a small cloud cover (<10%). EnMAP data can be accessed by submission of an acquisition request through the EnMAP Instrument Planning portal (<https://planning.enmap.org>).

It is equipped with a passive push-broom type hyperspectral imager (HSI) that records reflected radiation between 420 nm to 2450 nm in 246 bands,

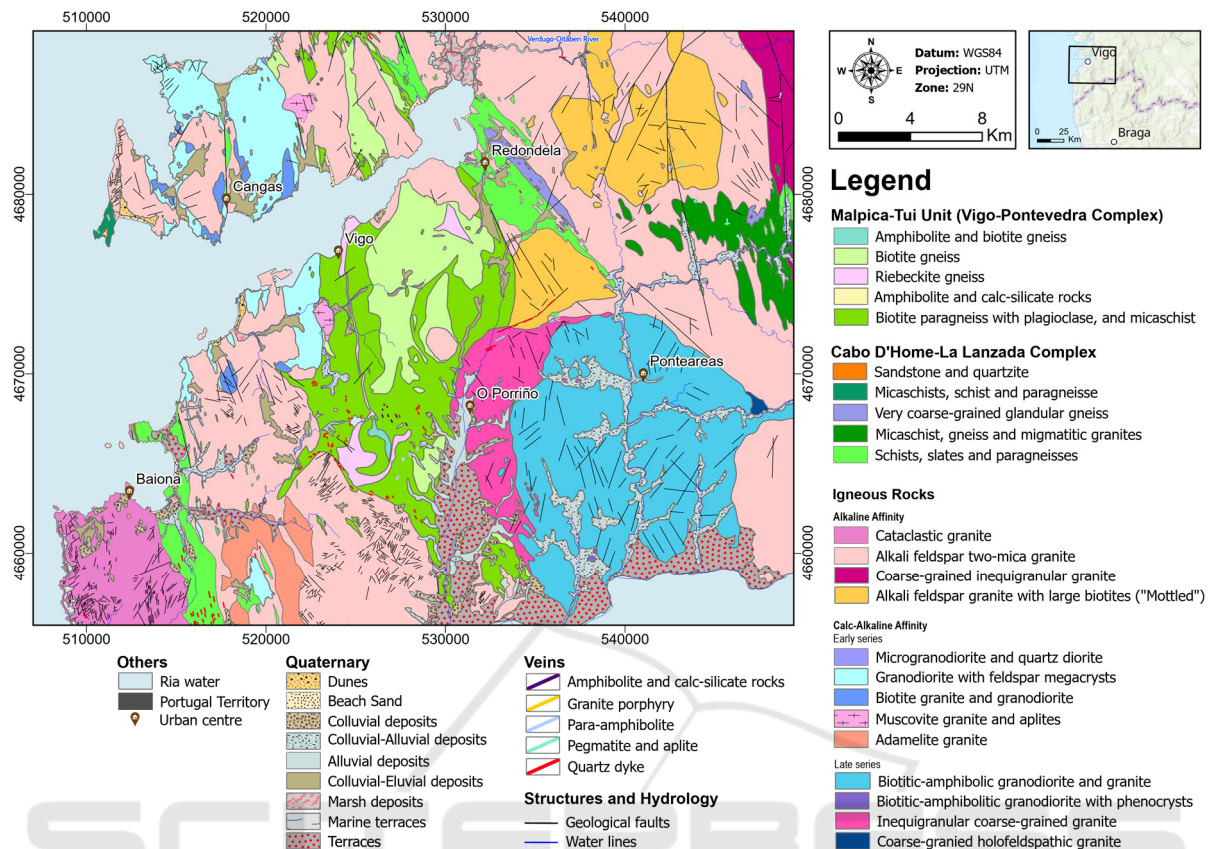


Figure 2: Geological map of the study area, based on the MAGNA 50 – Geological map of Spain, at scale 1:50000.

covering the Visible-Near Infrared (NIR) and the Short-Wave Infrared (SWIR) range of the electromagnetic spectrum (Storch et al., 2023). The spectral resolution is 6.5 nm in the VNIR range and 10 nm in the SWIR, while the spatial resolution is 30 m, providing a swath width of 30 km (Guanter et al., 2016).

3.2 Processing

EnMAP was processed using two platforms: the Sentinel Application Platform (SNAP) and the Environment for Visualising Images (ENVI) 6.0. EnMAP's L2A products are considered analysis-ready, so no further processing is needed except for spectral subsetting to remove bad-quality bands, which are corrupted data layers containing no data pixels (Alicandro et al., 2022). In this case, bands number 131 (1342.82 nm), 132 (1354.76 nm), 133 (1366.69 nm), 134 (1378.60 nm) and 135 (1390.48 nm) were manually identified and removed. As a result, the final product consists of 219 bands out of the original 224.

3.2.1 Band Ratios

For mineral mapping, band ratios were performed in the first instance to detect zones of alteration and possible mineralisation.

Different band ratios were tested in this work to highlight areas of possible hydrothermal alteration, mainly several ratios for clay minerals, iron oxides and silicates, as well as carbonates. Hydrothermal alteration zones in coastal zones can indicate potential source areas for HM (cassiterite, gold, etc).

Henrich et al. (2012) previously defined several band ratios, which can be consulted at <https://www.indexdatabase.de/>. These ratios are described in Table 1.

3.2.2 Spectral unmixing

The Mixture Tuned Matched Filtering (MTMF) algorithm was employed to detect specific mineral signatures within the image through a spectral unmixing approach. The MTMF supervised classification is based on partial unmixing since it can unmix an endmember from an unknown background.

Table 1: Description of the band ratios performed.

Band ratio	Type of mineral featured
$\frac{153}{189}$	Alteration
$\frac{(153 + 196)}{189}$	Alunite/Kaolinite/Pyrophyllite
$\frac{189 * 204}{196^2}$	Clay
$\frac{204}{189}$	Kaolinite
$\frac{(204 + 217)}{208}$	Carbonate/Chlorite/Epidote
$\frac{(196 + 217)}{(204 + 208)}$	Epidote/Chlorite/Amphibole
$\frac{46}{29}$	Ferric iron
$\frac{189}{68} + \frac{29}{45}$	Ferrous Iron
$\frac{153}{68}$	Ferric Oxides
$\frac{189}{153}$	Ferrous Silicates
$\frac{187 + 197}{194}$	Al-sheetsilicates
$\frac{196}{208}$	Amphibole
$\frac{196 + 217}{208}$	Amphibole/ MgOH

It uses a Matched Filter (MF) to match the known spectral signature to the image spectra, maximising the response of the target spectra and suppressing the response of unknown elements in the image (Kumar et al., 2022). The result is a target abundance image where each pixel has an MF score. The other part of the classification consists of applying a Mixture Tuning (MT) method to reduce false positives by using a linear spectral mixing model to add an infeasibility image to the results. The results are a set of rule images that correlate to the MF and infeasibility scores, for each pixel, when compared to each endmember spectra. In this work, endmembers were selected from two different spectral libraries, one used for each classification attempt (Table 2).

Table 2: Independent spectral libraries used for the MTMF classification and description of the endmembers.

First Classification (USGS library)	Second Classification (HM library)	
	Spectrum code	Manual interpretation
Almandine	UPO_1	Montmorillonite, Illite
Goethite	UPO_2	Amphibole, Montmorillonite
Grossular	UPO_3	Amphibole, Montmorillonite
Ilmenite	UPO_4	Amphibole, Montmorillonite
Monazite	UPO_5	Chlorite, Biotite
Rutile	UPO_6	Montmorillonite, Illite
Sillimanite	UPO_7	Tourmaline, Garnet
Spessartine	UPO_8	Tourmaline, Garnet
Tourmaline	UPO_9	Tourmaline, Garnet
Zircon	UPO_10	Tourmaline, Garnet

The first spectral library was derived from the USGS spectral library (Kokaly et al., 2017), and the minerals that constitute the endmembers were selected due to their known occurrence in the Ria de Vigo. The second was obtained in the scope of the S34I project, where HM concentrates of Vigo beach placer samples were collected in a laboratory, and their spectral signature was identified with an ASD FieldSpec4 spectroradiometer. While these HM concentrates are not spectrally pure, they were used as endmembers since they represent the mix of materials found in Vigo beaches.

4 RESULTS

4.1 Band Ratios

The best results were achieved with the Alteration, Ferric oxides and Amphibole band ratios (Fig. 3). The alteration band ratio successfully identified areas known to be affected by metamorphism and, therefore, more likely to have significant

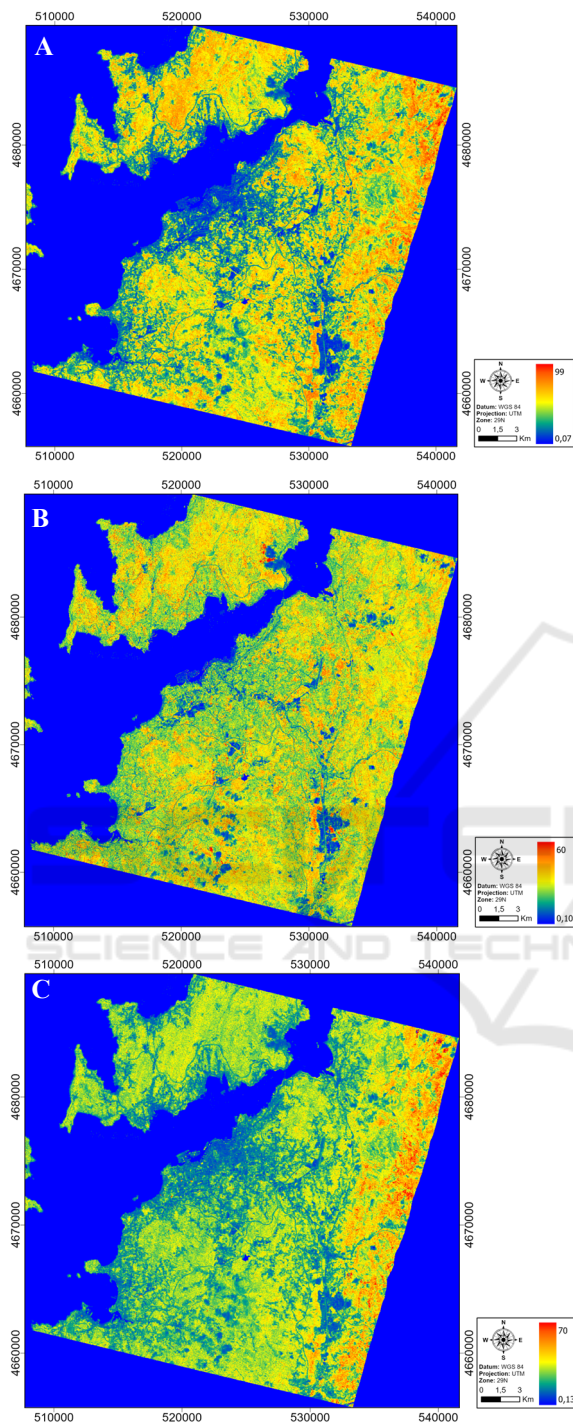


Figure 3: A) Alteration band ratio; B) Ferric oxides band ratio; C) Amphibole band ratio.

hydrothermal alteration. These areas are characterised by the vast presence of granitoids, which, through chemical weathering, lead to the formation of clay minerals. The ferric oxide ratio shows a relatively uniform distribution throughout

the image, with a slight increase in ferric oxides within igneous rock formations. Finally, the Amphibole band ratio displayed higher values (corresponding to warmer colours) in areas where amphibolitic rocks are known to outcrop.

Band ratios were useful for identifying broad areas of interest despite the limits imposed by the dense vegetation across the entire EnMAP image area.

4.2 Spectral Unmixing - MTF

For both MTF classifications, two distinct maps were produced using the Rule Classifier incorporated in the ENVI software. The maps contain all identified endmembers, each class represented by a different colour. The classification maps were performed for Límens-Santa Marta, Vao-Samil, Patos and Alemáns-Ratas-Canabal beaches (Fig. 4).

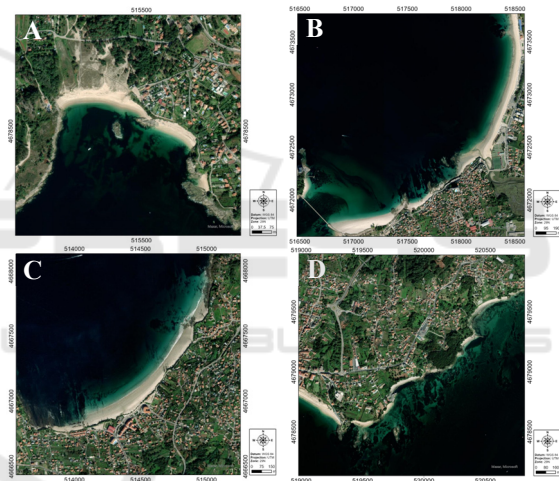


Figure 4: ESRI Basemap imagery for all target Vigo beaches; A – Límens-Santa Marta beaches; V- Vao-Samil beaches; C – Patos beach; D – Alemáns-Ratas-Canabal beaches.

In the first classification, using the USGS spectral library (Fig. 5), several mineral signatures were identified across the Vigo beaches, being the main ones Límens-Santa Marta and Vao. In the Límens-Santa Marta beaches, signatures from rutile, goethite, sillimanite, tourmaline, and all three varieties of garnet, almandine, grossular, and spessartine, were identified. Spessartine and rutile are mostly present in dunes. At the Vao beach, sillimanite and grossular signatures were more dominant. On the Vao and Samil beaches boundary, ilmenite and tourmaline were classified on rock outcrops. Iron oxides were found to be more abundant at Límens-Santa Marta.

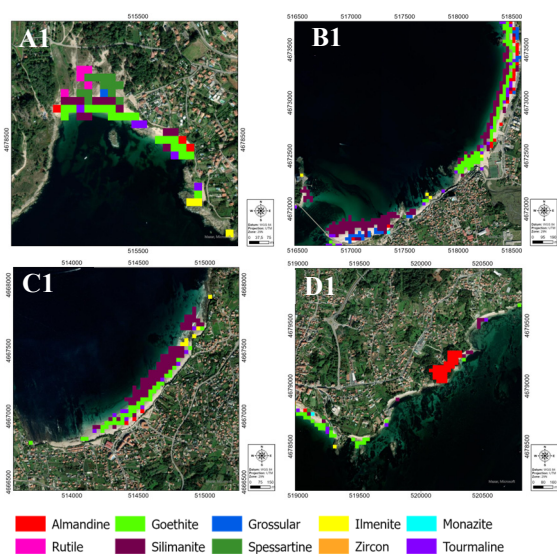


Figure 5: Classification maps derived from the first MTMF classification using the USGS spectral library and comparison between Límens-Santa Marta (A1), Vao-Samil (B1), Patos (C1) and Alémans-Ratas-Canabal (D1) beaches.

At Patos beach, the goethite signature appears in higher abundance, especially when compared to Vao beach. Sillimanite was the most abundant mineral signature along the stretch that includes Alemáns-ratas-Canabal beaches.

Using the spectra from HM concentrations for the second classification (Fig. 6), the most abundant endmember identified in the Límens-Santa Marta beaches is UPO_1 (montmorillonite). Other significant endmembers include UPO_2, UPO_3 and UPO_4, which are interpreted to be amphibole (possibly hornblende), with the differential identification of montmorillonite), as well as UPO_5, likely corresponding to chlorite/biotite. A smaller abundance of UPO_6 (montmorillonite) was also identified.

At the Vao beach, UPO_1 is present but in a much lower abundance, with it increasing along the transition northward to the Samil beach. UPO_2 and UPO_3 are also present, and UPO_9 (tourmaline/garnet) can be observed in rock outcrops.

Patos beach exhibits a high abundance of UPO_1 (montmorillonite/illite), while in Alemáns-Ratas-Canabal beaches, the same trend continues, with UPO_1 and UPO_4 (amphibole) being the most abundant endmembers.

Seasonal variations previously described can be seen in the MTMF classifications since the highest abundance of goethite was found in Límens-Santa Marta beaches in the northern margin.

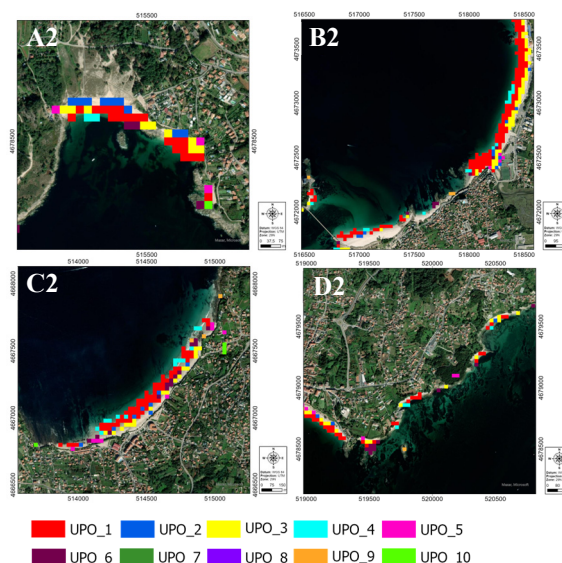


Figure 6: Classification maps derived from the second MTMF classification using the HM concentrate spectral library and comparison between Límens-Santa Marta (A2), Vao-Samil (B2), Patos (C2) and Alémans-Ratas-Canabal (D2) beaches.

5 CONCLUSIONS

EnMAP data, due to its high spectral resolution, was essential to distinguish several HM signatures in the Vigo beaches. Band ratios are mostly useful for the detection of potential areas of primary mineralisation, due to evidence of hydrothermal alteration signatures. When combined with other datasets, these maps could help understand the provenance of HM in placers. Spectral unmixing, included in the MTMF workflow, identified signatures from most HM known to be present in the Vigo beaches, except zircon. Límens-Santa Marta and Vao beaches have the highest abundance of HM, being the signature of sillimanite the most identified, although likely to be overrepresented. Garnets (almandine, grossular and spessartine), tourmaline, ilmenite signatures were also identified. Goethite signature is more abundant in Límens-Santa Marta beach due to seasonal variations in the Ria's hydrodynamics. In future works, exploring fusion methods of EnMAP and Sentinel-2 data may be of value to enhance EnMAP's spatial resolution. Additionally, ground truth data may be collected to determine MTMF's accuracy in classifying and identifying HM in the Vigo beaches.

ACKNOWLEDGEMENTS

This study is funded by the European Union under grant agreement no. 101091616 (<https://doi.org/10.3030/101091616>), project S34I – SECURE AND SUSTAINABLE SUPPLY OF RAW MATERIALS FOR EU INDUSTRY. Portuguese National Funds also support this work through the FCT – Fundação para a Ciência e a Tecnologia, I.P. (Portugal), projects UIDB/04683/2020 (<https://doi.org/10.54499/UIDB/04683/2020>) and UIDP/04683/2020 (<https://doi.org/10.54499/UIDP/04683/2020>).

REFERENCES

- Alicandro, M., Candigliota, E., Dominici, D., Immordino, F., Masin, F., Pascucci, N., Quaresima, R., & Zollini, S. (2022). Hyperspectral PRISMA and Sentinel-2 Preliminary Assessment Comparison in Alba Fucens and Sinuessa Archaeological Sites (Italy). *Land*, 11, 2070. <https://doi.org/10.3390/land11112070>
- Capdevila, R., & Floor, P. (1970). Les différents types de granites hercyniens et leur distribution dans le nord ouest de l'Espagne. *Boletín Geológico y Minero. T. LXXXI.-II-III Año*, 215, 225.
- Chandrasekar, N., Mujabar, P. S., & Rajamanickam, G. V. (2011). Investigation of heavy-mineral deposits using multispectral satellite data. *International Journal of Remote Sensing*, 32(23), 8641-8655. <https://doi.org/10.1080/01431161.2010.545448>
- European Commission, Directorate-General for Internal Market, I., Entrepreneurship, SMEs, Grohol, M., & Veeh, C. (2023). *Study on the critical raw materials for the EU 2023 – Final report*. Publications Office of the European Union. <https://data.europa.eu/doi/10.2873/725585>
- Galván, F. M. (2002). Exploración de placeres costeros de minerales pesados y su génesis en la costa de Galicia.
- Gazi, M., Taphim, K., Ahmed, M. K., & Islam, M. A. (2019). Investigation of heavy-mineral deposits using multispectral satellite imagery in the eastern coastal margin of Bangladesh. *Earth Science Malaysia*, 3, 16-22. <https://doi.org/10.26480/esmy.02.2019.16.22>
- Gent, M., Alvarez, M., García Iglesias, J., & Álvarez, J. (2005). Offshore Occurrences of Heavy-Mineral Placers, Northwest Galicia, Spain. *Marine Georesources & Geotechnology - MAR GEORESOURCES GEOTECHNOL.*, 23, 39-59. <https://doi.org/10.1080/10641190590959939>
- Guanter, L., Kaufmann, H., Förster, S., Brosinsky, A., Wulf, H., Bochow, M., Boesche, N. K., Brell, M., Buddenbaum, H., Chabrillat, S., Hank, T. B., Heiden, U., Hill, J., Heim, B., Heldens, W., Hollstein, A., Hostert, P., Krasemann, H., Leitão, P. J., ... Oppelt, N. (2016). EnMAP Science Plan.
- Henrich, V., Krauss, G., Götze, C., & Sandow, C. (2012). IDB - www.indexdatabase.de, Entwicklung einer Datenbank für Fernerkundungsindizes. In A. Fernerkundung (Ed.). Bochum.
- Hool, A., Helbig, C., & Wierink, G. (2023). Challenges and opportunities of the European Critical Raw Materials Act. *Mineral Economics*.
- IGME. (1976). Investigación minera preliminar de la plataforma continental submarina de la costa gallega. In *Programa sectorial de Estudio de Fondos Marinos (FOMAR)*. Ministerio de Industria.
- Julivert, M., Fontboté, J. M., Conde, L., Aldaya, F., Capdevila, R., Delgado Quesada, M., Marcos, A., Rosell, J., Soler, M., Den Tex, E., Tamain, G., Mointinho de Almeida, F., Zbyszewski, G., Manupella, G., & Carvalhosa, A. (1974). *Mapa tectónico de la península Ibérica y Baleares a escala 1:1.000.000 y memoria explicativa*. Instituto Geológico y Mineiro de España.
- Kokaly, R. F., Clark, R. N., Swayze, G. A., Livo, K. E., Hoefen, T. M., Pearson, N. C., Wise, R. A., Benz, W. M., Lowers, H. A., Driscoll, R. L., & Klein, A. J. (2017). USGS Spectral Library Version 7.
- Kumar, V., Pandey, K., Panda, C., Tiwari, V., & Agarwal, S. (2022). Assessment of Different Spectral Unmixing Techniques on Space Borne Hyperspectral Imagery. *Remote Sensing in Earth Systems Sciences*, 5. <https://doi.org/10.1007/s41976-022-00071-8>
- Méndez, G., Rey García, D., Bernabeu Tello, A. M., Manso Galván, F., & Vilas Martín, F. (2000). Recursos minerales marinos en las rías gallegas y en la plataforma continental adyacente. *Journal of Iberian geology: an international publication of earth sciences*, 26, 67-98. <https://portalcientifico.uvigo.gal/documentos/5f92241529995257a670d7a0>
- Méndez, G., & Vilas, F. (2005). Geological antecedents of the Rias Baixas (Galicia, northwest Iberian Peninsula). *Journal of Marine Systems*, 54(1), 195-207. <https://doi.org/https://doi.org/10.1016/j.jmarsys.2004.07.012>
- Navas, J. R., & Corretgé, L. (1997). *Hoja 223 (Vigo) - Mapa Geológico de España, Escala 1:50.000*. Madrid, Instituto Geológico y Minero de España.
- Ng-Cutipa, W. L., Lobato, A., González, F., Georgalas, G., Zananiri, I., Cardoso-Fernandes, J., Carvalho, M., Azzalini, A., Araújo, B. L., & Teodoro, A. C. (2024). *Airborne images integration for a first cartographic approximation of critical raw-materials-rich placers on Santa Marta Beach (Ría de Vigo, NW Spain)* (Vol. 13197). SPIE. <https://doi.org/10.1117/12.3031637>
- Pérez, I. P., Bernabéu, A. M. G., Rey, D., & Vilas, F. (2008). Formación del placer de la playa de Montalvo (Pontevedra).
- Prego, R., Caetano, M., Vale, C., & Marmolejo-Rodríguez, J. (2009). Rare earth elements in sediments of the Vigo Ria, NW Iberian Peninsula. *Continental Shelf Research*, 29, 896-902. <https://doi.org/10.1016/j.csr.2009.01.009>
- Rejith, R. G., Sundararajan, M., Lakshmanan, G., & Loveson, V. (2020). Satellite-based spectral mapping (ASTER and landsat data) of mineralogical signatures of beach sediments: a precursor insight. *Geocarto*

International, 37, 1-24. <https://doi.org/10.1080/10106049.2020.1750061>

Rejith, R. G., Sundararajan, M., Lakshmanan, G., Seenipandian, & Chandrasekar, N. (2022). Exploring beach placer minerals in the east coast of Tamil Nadu, India, using EO-1 Hyperion data. *Journal of Applied Remote Sensing*, 16. <https://doi.org/10.1117/1.JRS.16.012017>

Storch, T., Honold, H.-P., Chabrilat, S., Habermeyer, M., Tucker, P., Brell, M., Ohndorf, A., Wirth, K., Betz, M., Kuchler, M., Mühle, H., Carmona, E., Baur, S., Mücke, M., Löw, S., Schulze, D., Zimmermann, S., Lenzen, C., Wiesner, S., . . . Fischer, S. (2023). The EnMAP imaging spectroscopy mission towards operations. *Remote Sensing of Environment*, 294, 113632. <https://doi.org/https://doi.org/10.1016/j.rse.2023.113632>

